Materials Science and Engineering A xxx (2010) xxx–xxx

Contents lists available at ScienceDirect

Materials Science and Engineering A

journal homepage: www.elsevier.com/locate/msea

Mechanical experiments on the superplastic material ALNOVI-1, including leak information

Q.H.C. Snippe*, T. Meinders

National Institute for Subatomic Physics (Nikhef), Engineering Department, PO Box 41882, Amsterdam, the Netherlands

ARTICLE INFO

Article history:
Received 30 October 2009
Received in revised form 9 September 2010
Accepted 10 September 2010
Available online xxx

Keywords:
Superplastic forming
Mechanical experiments
ALNOVI-1

ABSTRACT

In subatomic particle physics, unstable particles can be detected with a so-called vertex detector, placed inside a particle accelerator. A detecting unit close to the accelerator bunch of charged particles must be separated from the accelerator vacuum. A thin sheet with a complex 3D shape prevents the detector vacuum from polluting the accelerator vacuum. Therefore, this sheet has to be completely leak tight. However, this can conflict with restrictions concerning maximum sheet thickness of the product. To produce such a complex thin sheet, superplastic forming can be very attractive in cases where a small number of products is needed. In order to predict gas permeability of these formed sheets, many mechanical experiments are necessary, where the gas leak has to be measured. To obtain insight in the mechanical behaviour of the used material, ALNOVI-1, tensile experiments were performed to describe the uniaxial stress–strain behaviour. From these experiments, a high strain rate sensitivity was measured. The flow stress of this material under superplastic conditions was low and the material behaved in an isotropic manner upon large plastic strains. The results of these experiments were used to predict the forming pressure as a function of time in a free bulge experiment, such that a predefined target strain rate will not be exceeded in the material. An extra parameter within these bulging experiments is the application of a hydrostatic pressure during the forming process. Such a pressure postpones the nucleation and growth of internal cavities, which means that higher plastic strains can be reached before failure. Results from these experiments showed that at higher hydrostatic pressures, higher bulges were made. All these bulges were leak tested, showing also that higher hydrostatic pressures lead to a lower void volume fraction at higher hydrostatic pressures, since these bulges were more leak tight at the same bulge height than bulges made without the application of this pressure. This article describes the setup and results of the uniaxial (tensile) and biaxial (bulging) experiments on the superplastic aluminium ALNOVI-1.

1. Introduction

Superplastic materials show a very high sensitivity in mechanical properties with respect to the strain rate, especially the flow stress is largely determined by the strain rate sensitivity. The mechanical property description of a superplastic material is sometimes described by a simple formulation where only the strain rate serves as the input for a flow stress calculation, e.g. as in [1], and also used in, e.g. [2–4].

$$\sigma_f = k\dot{\varepsilon}^m \tag{1}$$

where σ_f is the flow stress, k is a material constant, $\dot{\varepsilon}$ is the equivalent plastic strain rate and m is an exponent representing the strain rate sensitivity. Far more complex models are used [5–9], depending on the desired type of results and accuracy, and they can be classified into two categories [1]. First, a physical material model can be used where all input parameters can directly be coupled to the deformation mechanism of the material. These, mostly micromechanical, models use input parameters like activation energies or dislocation densities [10,11], which are relatively difficult to extract from mechanical experiments. The second category covers the phenomenological material description [12]. Depending on the amount of variables to describe the properties, such a description can be very accurate. The input parameters generally do not have a physical connection with the material.

In order to extract the desired material properties in case of a phenomenological model, several types of experiments are necessary. Tensile tests are used to determine stress–strain relationships. Bulge experiments determine the basis for biaxial flow behaviour. In this research, the superplastic aluminium alloy ALNOVI-1 has been selected [13] for the following two reasons. First, a formed sheet with a complex 3D shape has to meet two conflicting requirements, when used in certain applications inside a particle detector. These are formulated in a minimisation of the resulting thickness of the formed sheet, and a minimisation of the leak tightness of this sheet. Therefore, it may be beneficial if the initial sheet thick-

* Corresponding author. Tel.: +31 205922105; fax: +31 205925155.
E-mail address: csnippe@nikhef.nl (Q.H.C. Snippe).

0921-5093/$ – see front matter © 2010 Elsevier B.V. All rights reserved.
doi:10.1016/j.msea.2010.09.075

Table 1
Chemical composition of ALNOVI-1.

Mg	Mn	Cr	Fe	Si	Al
4.5	0.7	0.12	<0.1	<0.1	Bal.

ness is already low. ALNOVI-1 is a material which is available in thin sheets, 0.3 mm being the smallest thickness, where most superplastic sheet manufacturers do not have sheets thinner than 1.0 mm. Secondly, from the formed gas barrier sheets, only a few products are needed. This justifies the use of ALNOVI-1, since this material can be obtained in relatively small batches. The chemical composition of this material is given in Table 1.

The purpose of the experiments presented in this article is mainly to obtain insight in the mechanical behaviour of ALNOVI-1. Uniaxial tensile experiments are used to derive stress–strain behaviour as function of the strain rate. This stress–strain behaviour is then used as an input to design the biaxial, free bulging experiments [14–17]. These experiments were carried out to observe the biaxial behaviour, where the leak tightness is the most important property. The amount of leak was measured with a helium leak tester in a separate setup, apart from the free bulging setup. Since superplastic materials show their optimal superplasticity within a narrow strain rate range, it is of crucial importance that the forming pressure in a bulging experiment should be applied in time, such that a predefined target strain rate will not be exceeded anywhere in the model [18,19]. Other authors confirm this procedure [20,21].

Section 2 describes the setup and results of the uniaxial, tensile experiments carried out on ALNOVI-1. From these experiments, a set of stress–strain curves is derived by means of inverse modelling (simulation of the experiment), see Section 3. This stress–strain behaviour is then used in combination with a strain rate controlling program to calculate the pressure progress in time to be used in the free bulging experiments. These experiments are the subject of Section 4.

One of the most important properties to know about the material in the application is the permeability of the deformed material with respect to gases. This is caused by the formation of internal cavities [22,23]. Before the material fails by fracture, enough voids may have been formed, grown, or may even have been interlinked, to provide a leak channel through the thickness of the formed material.

To delay the formation of voids, a hydrostatic pressure can be applied during the test [24], where it is concluded that the application of such a pressure influences the void nucleation and growth, but not the superplastic deforming mechanism, i.e. grain boundary sliding (GBS). The influence of this backpressure on the mechanical behaviour can be studied. Section 5 is dedicated to the gas permeability measurements of the formed bulges. The purpose of these experiments is to extract material parameters in order to build a material model which can be used in superplastic forming simulations.

2. Uniaxial experiments

Tensile tests are used to extract uniaxial stress–strain data. They are carried out on a Hounsfield tensile testing machine, equipped with a tunnel furnace. The cross-head velocity of the tensile bar can vary between 1 and 999 mm/min. This value cannot be changed during a test. A thin copper wire has to prevent the specimen from falling off the tensile bars once the test starts.

2.1. Specimen geometry

The dimensions of the tunnel furnace largely determine the geometry of the tensile specimens. The length of the effective zone must be found as a compromise between these furnace dimensions and the expected elongation, thereby prescribing a maximum specimen length. On the other hand, minimising the strain rate prescribes certain minimum dimensions: the larger the effective length, the smaller the strain rate with equal cross-head velocity. The effective length of the specimen, excluding the 2 mm radius fillets, is 12 mm, see Fig. 1. The specimen thickness is 0.8 mm.

At a cross-head velocity of 1 mm/min, this would result in a strain rate of about 0.001 s^{-1}, if all of the tensile bar displacement could be dedicated to the deformation of this effective zone. There are more factors which can influence the strain rate, such as an elongation of the connection holes to the tensile bar. The tensile specimens are manufactured by Electro-Mechanic Discharge (EMD). This process is able to create smooth surfaces without too many burrs. It is also a process which does not create a heat affected zone, as is the case with, e.g. laser cutting.

2.2. Performed tensile tests

Two types of tensile experiments were done in order to extract all the necessary output. First, destructive tensile tests at different velocities provided information concerning the stress–strain behaviour at different strain rates. Secondly, non-destructive tests were carried out where each test was stopped at a prescribed load. The purpose of these tests is to study the dependence of the void volume fraction with respect to the plastic strain and strain rate, and also to obtain insight in the (an-)isotropy of the material.

The temperature range for optimal superplasticity is very small, values are reported varying between 500 and 530 °C, see [3,4]. Fig. 2 shows the typical load–displacement curves coming from a first set of experiments, the optimal superplastic temperature for the material ALNOVI-1 was found to be 520 °C. All experiments were started 10 min after the target temperature had been reached.

The destructive tensile tests were performed at five different speeds ranging from 1 to 10 mm/min, at three different orientations with respect to the material drawing direction: parallel, perpendicular and at a 45° angle. Taking into account the micromechanical superplastic deforming mechanism, which is mainly the effect of Cooperative Grain Boundary Sliding (CGBS, see [5]), it was to be expected that the material is planar isotropic.

The second type of experiments concerns non-destructive tests. It is known that internal voids will nucleate and grow inside the material with increasing plastic strain. To investigate this relationship, tensile experiments should be carried out until a prescribed value of the strain (elongation). Since, from Fig. 2, it is clear that the force decreases approximately linearly over a large elongation range, it was decided to carry out experiments until some predefined fractions of the maximum force measured during the test. At

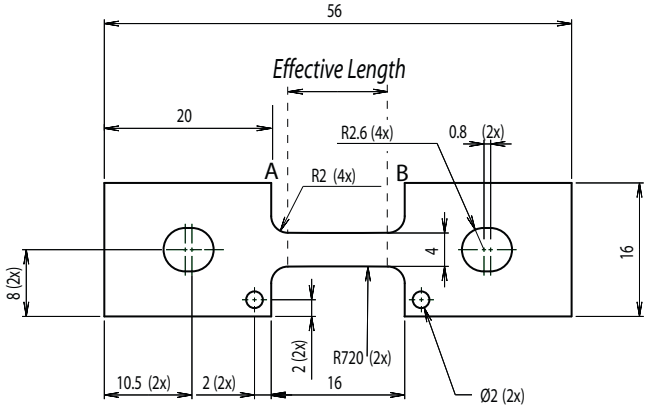

Fig. 1. Tensile specimen geometry.

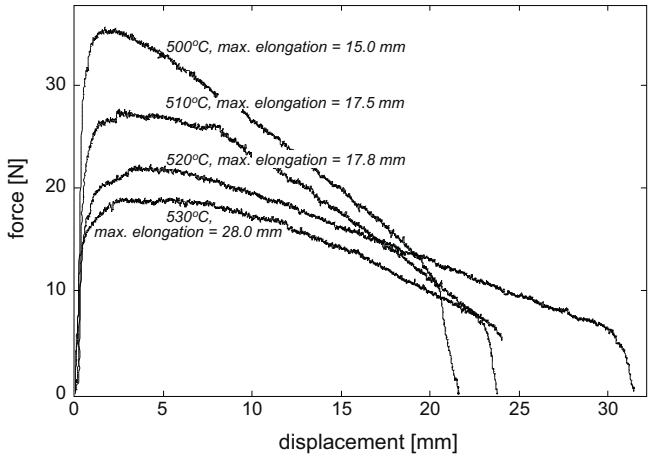

Fig. 2. Force–displacement curves at 2 mm/min at different temperatures. Each test has been repeated two times. Elongation has been measured as the distance increase between the points A and B in Fig. 1.

three different cross-head velocities, experiments were done until the force has been dropped till a percentage of the maximum force measured in the corresponding destructive tests.

2.3. Tensile test results

The results of the uniaxial tests will be presented in this section where, in case of the destructive experiments, the force–displacement data are presented. In case of the non-destructive experiments, the void growth behaviour was studied. Also, the strain in width and thickness direction was measured from the non-destructive tests, giving Lankford's strain ratio.

2.3.1. Destructive tensile tests

The destructive tests in which the specimens were all loaded until fracture, resulted in force–displacement curves for a set of five different cross-head velocities. It can be observed that the forces are very low compared to results usually obtained in tensile tests on aluminium specimens. Fig. 3(a) shows the force–displacement curves of the test specimens in rolling direction for five different tensile velocities. From this figure, the high strain rate sensitivity becomes apparent as there is much difference between the curves at different drawing velocities. Fig. 3 (b) shows the load–displacement curves for the tensile velocity of 2 mm/min, for all three loading directions, showing the (an-)isotropy of the material. Until a displacement of 24 mm, the material can be considered planar isotropic. If the displacement exceeds this value, the three loading directions result in planar anisotropic behaviour, as can be seen in the way the three curves deviate from each other. It is supposed that at higher strains, the Grain Boundary Sliding becomes relatively more difficult, which is caused by grain growth and void formation. Therefore, conventional plastic behaviour can take part in the overall deformation process, making the material anisotropic.

2.3.2. Non-destructive tensile tests

To study the void volume fractions in the drawn specimens, they were polished and investigated under a light microscope. Electron microscope observations are also possible, but this gives so much detail and focus depth, that there is not much contrast between void and material and thus it would be very hard to estimate the void volume fraction. The width and thickness of the specimens, leading to values for width and thickness strain, are also a measure for the amount of anisotropy of the material, expressed in the Lankford strain ratio. This ratio is determined as the strain in width

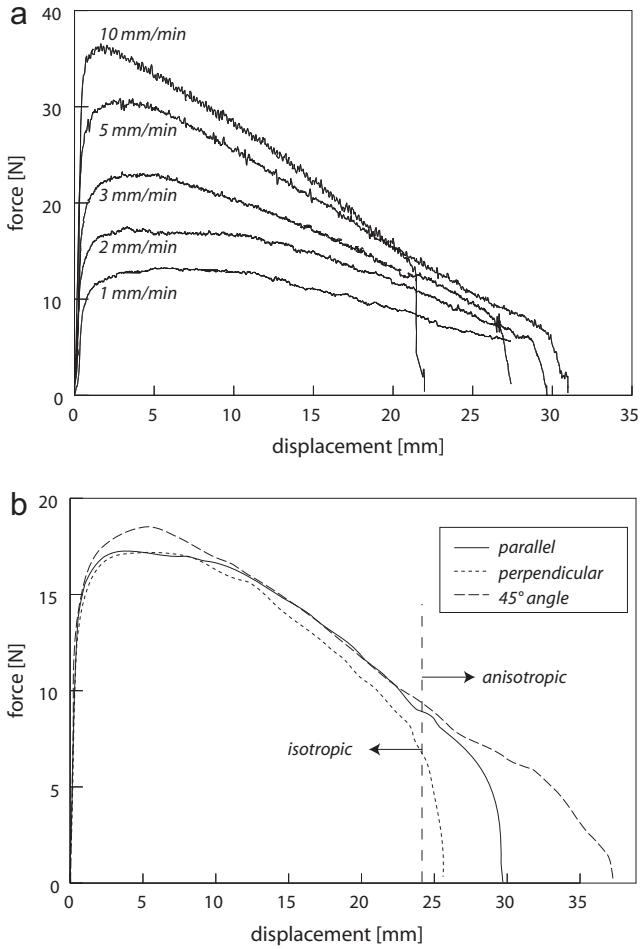

Fig. 3. Force–displacement curves at different tensile velocities (a), and the same curves at 2 mm/min for three loading directions (b).

direction divided by the thickness strain in a uniaxial experiment. A value less than 1, which is common for aluminium alloys, means that the absolute value plastic thickness strain is higher than the absolute plastic strain in the in-plane direction perpendicular to the loading direction. Table 2 shows the R values in three directions, together with the average strain ratio $\bar{R}$ and the sensitivity ΔR to the loading direction. This number is very low (absolute value smaller than 0.005), meaning that the material can be considered planar isotropic.

Fig. 4 shows the typical void growth behaviour in ALNOVI-1 with increasing plastic strain.

2.4. Void volume fractions

As mentioned in Section 2.2, the non-destructive tests were stopped at a prescribed value of the tensile force. This tensile force in time turned out to be highly reproducible. The tests were performed at tensile velocities of 1, 3 and 10 mm/min. At each velocity, the test was stopped at 60, 40, 30, 20 and 10% of the maximum drawing force. To obtain an accurate view of the internal cavities and to calculate the void volume fraction, the specimens have to be

Table 2
Lankford strain ratios of ALNOVI-1, including average strain ratio $\bar{R}$ and the amount of anisotropy, expressed in ΔR.

R_0	R_{45}	R_{90}	$\bar{R}$	ΔR
0.816	0.827	0.829	0.825	−0.0043

Please cite this article in press as: Q.H.C. Snippe, T. Meinders, Mater. Sci. Eng. A (2010), doi:10.1016/j.msea.2010.09.075

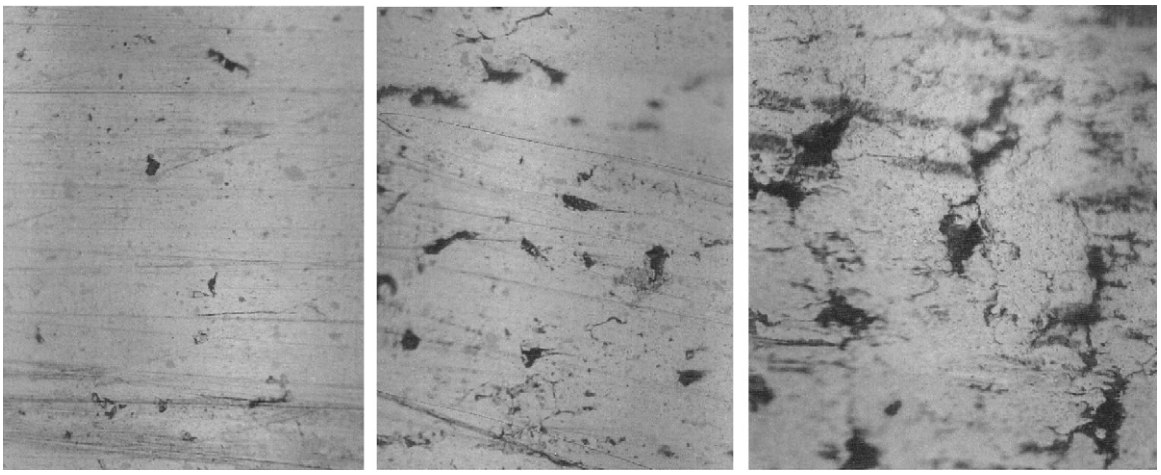

Fig. 4. Picture of void growth in ALNOVI-1 with increasing plastic strain: $\varepsilon^p = 0.1$, $\varepsilon^p = 0.9$ and $\varepsilon^p = 1.3$.

polished thoroughly. This ensures a sharp edge between the surface and the cavity, which can be used in photo editing software to count the amount of cavity pixels with respect to the total amount of pixels. The ratio between these two numbers defines the void area fraction ξ_a.

The void volume fraction ξ_v is related to the void area fraction ξ_a by Eq. (2). It is assumed that the void area fraction is independent on the orientation of the observed plane.

$$\xi_v = 1 - (1 - \xi_a)^{3/2} \tag{2}$$

In Fig. 5, the void volume fractions are presented as function of the equivalent plastic strain for different strain rates. First, as was also shown qualitatively in Fig. 4, the void volume fraction increases with increasing plastic strain. Secondly, the void volume fraction shows hardly any dependence on the strain rate. Thirdly, it seems that there is a transition value for the plastic strain ε_{tr}, where the void volume fraction rate increases instantly, from $\dot{\xi}_1$ to $\dot{\xi}_2$.

2.5. Strain rate sensitivity

Eq. (1), which describes superplasticity in its most basic form, is only valid within a small range of equivalent plastic strain rate. The value of m is however not constant and depends on this strain rate. Several methods of calculating the strain rate sensitivity exist, see for instance [25], where four different methods are discussed. A general expression for the calculation of the strain rate sensitivity is used in these methods, which is

$$m = \frac{\ln(\sigma_2/\sigma_1)}{\ln(\dot{\varepsilon}_2/\dot{\varepsilon}_1)} \tag{3}$$

where the subscripts 1 and 2 refer to two different loading rates. Since the stress is also dependent on the plastic strain, and not on the strain rate only, the value of m is not constant for a given strain rate. The choice made is to calculate the strain rate sensitivity based on the maximum tensile load in the specimens, i.e. the maxima of the curves given in Fig. 3. This results in the values for m as given in Table 3. In the table, strain rate values are given, the method of determining will be explained in more detail in Section 3.

The highest strain rate sensitivity is seen between a tensile velocity of 2 and 3 mm/min.

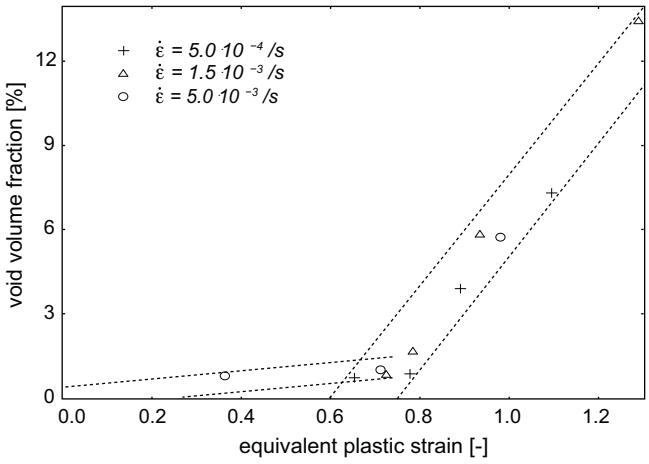

Fig. 5. Void volume fractions as measured from the non-destructive tensile experiments.

3. Mechanical behaviour

Since the strain rate range in which optimal superplasticity occurs is very small, it is important that a predefined target strain rate will not be exceeded in superplastic forming. To carry out bulge tests with a prescribed target strain rate (which should be the maximum strain rate in the product), the pressure on the sheet should be a function of time. In order to define this pressure–time function, the stress–strain behaviour of the material needs to be known. Therefore, stress–strain curves at different strain rates were constructed using the force–displacement results of the tensile tests. This was done by inverse modelling, where the tensile experiments have been simulated.

This section describes the way in which the results of the tensile experiments are used to design the bulge experiments. Fig. 6 shows a flow diagram, starting with the raw tensile experiment output, which is in terms of force–displacement curves. The bulge experiments should be designed such that if a pressure is applied on a sheet, a predefined target strain rate should not be exceeded anywhere in the material during forming.

Force data of the tensile experiment should be translated into stress data, thereby assuming the evolution of the current cross-

Table 3
Strain rate sensitivity values as calculated from the load–deflection curves. The label given in the top rule of the table refers to the lower value of the two strain rate values (in 10^{-4} s^{-1}) which are compared with each other.

Target strain rate	6	12	18	30
m	0.43	0.70	0.55	0.25

Please cite this article in press as: Q.H.C. Snippe, T. Meinders, Mater. Sci. Eng. A (2010), doi:10.1016/j.msea.2010.09.075

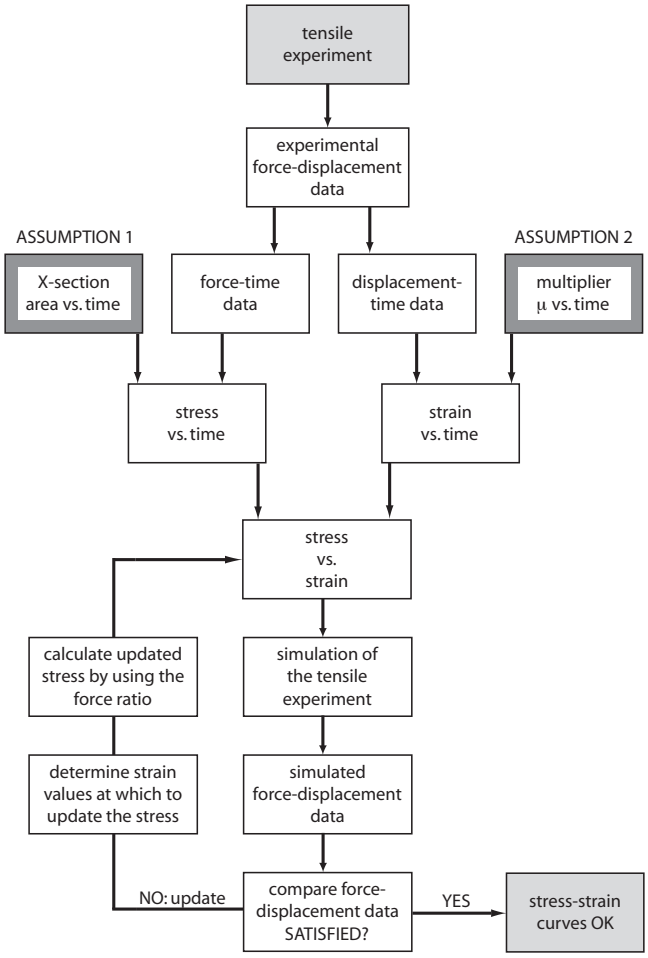

Fig. 6. Flow scheme explaining the method of transferring force–displacement curves from the tensile experiments into stress–strain data.

sectional area of the tensile specimen during straining. This will result in the stress evolution as a function of time.

Displacement data of the tensile experiment are used to estimate the current plastic strain in time. Not all of the displacement of the tensile bar can be attributed to the effective length of the specimen. A fraction of the tensile bar displacement should therefore be estimated in order to determine the change in effective length.

The estimated elongation of the effective length is then used to determine the plastic strain in this area. This results in the strain evolution as function of time.

The stress–time and strain–time relationships are then coupled to construct stress–strain curves at different strain rates. These strain rates are estimated from the constructed strain–time data. These stress–strain curves are used to perform an inverse modelling of the tensile tests: these are simulated with the constructed stress–strain data, where the output of these simulations is in terms of force versus displacement.

This force–displacement output is compared with the one measured in the experiments, the deviation between both is used to improve the stress–strain behaviour. The tensile force at 10 points on the simulated force–displacement curve is compared with the experimentally determined force at the same displacement. The strain at this displacement is then derived; this will be explained later in Section 3.1. The updated stress at this strain is then determined by multiplying the old stress value with the ratio between the experimentally and simulation-based force. This procedure is repeated until sufficient correspondence between the experiment and the simulation will be reached.

The construction of the stress–strain behaviour is the subject of Section 3.1. The stress–strain behaviour serves as an input to calculate the pressure on a sheet in the bulge experiments as function of time, this is descibed in Section 3.2.

3.1. Stress–strain behaviour

To estimate the stress in the tensile specimen as function of the time, the current cross-sectional area evolution must either be known, or estimated. Since it was not possible to monitor the width and thickness of the specimen during a tensile test, the cross-sectional area has to be estimated. The width and the thickness were measured at the start and the end of an experiment. The initial assumption of the cross-sectional evolution is such that both width and thickness decrease linearly with displacement (or time, since the tensile bar velocity is constant). As both the force and the estimated cross-sectional area with time are known, so is the estimated stress as function of time.

The estimate of the plastic strain is somewhat more complicated and a few assumptions have to be made. Since the flow stress is very low, it is assumed that all of the calculated strain can be considered plastic. The length of the effective zone is assumed to be 35% of the distance between the hole centers of the specimen, which is based on a purely elastic simulation. This fraction is taken as a starting value μ_0 at zero displacement, which increases with increasing strain. Also a first simulation, where only elasticity is considered, showed that initially approximately this fraction of the total displacement can be attributed to the effective zone.

The multiplier μ_x, which is initially 0.35, will increase with the overall displacement. Generally, in tensile experiments, the strain rate decreases with increasing elongation, provided that the tensile bar velocity is constant. However, in this case, the strain rate is assumed constant while constructing the stress–strain curves, because of this increase of μ_x with increasing elongation. If the drawing velocity is v [mm/s], then the strain rate is

$$\dot{\varepsilon} = \frac{\mu_0 v}{l_0} \tag{4}$$

where l_0 is the initial effective length, and μ_0 is the initial value of the multiplier. At the lowest tensile velocity, which is 1 mm/min, this results in an initial strain rate of $4.9 \times 10^{-4}\,s^{-1}$.

With this information and set of assumptions, five different stress–strain curves were constructed, each of them representing the experiments at one tensile bar drawing velocity from Fig. 3 (a). The resulting stress–strain curves are shown in Fig. 7(a) as the five dashed curves.

With this unidirectional material behaviour, the tensile experiments were simulated, leading to a set of five force–displacement curves. These *F–d* curves can be compared with the experimental ones, in order to improve the unidirectional material modelling.

From the simulations of each iteration, the following data can be extracted to update the input stress–strain curves. First, the equivalent plastic strain as function of time is known from the simulation. This means that the equivalent plastic strain rate is also known from the simulation, which can be compared with the assumption of a strain rate for each stress–strain curve. From the simulations it follows that the equivalent plastic strain rate in the effective zone is about 0 to 35% higher than estimated initially. That means that at a tensile velocity of 1 mm/min, the equivalent plastic strain rate, according to the simulation, decreases from $6.8 \times 10^{-4}\,s^{-1}$ at the onset of plastic strain to $5.0 \times 10^{-4}\,s^{-1}$ at the maximum plastic strain. This means that it is not necessary to redefine the stress–strain curves at other strain rates. Defining a material as a set of stress–strain curves at different strain rates are valid for the whole range of strain rates, and not only for the values at which these stress–strain curves are defined.

Please cite this article in press as: Q.H.C. Snippe, T. Meinders, Mater. Sci. Eng. A (2010), doi:10.1016/j.msea.2010.09.075

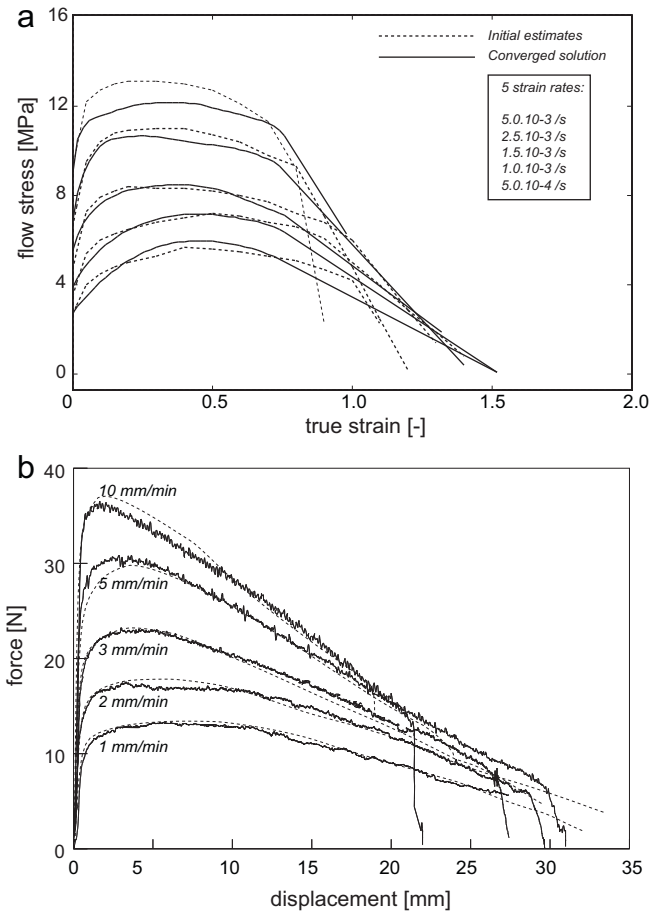

Fig. 7. Converged solution of the stress–strain behaviour after five iterations compared with the initial estimates (a), force–displacement curves of the simulations compared with the experimental ones for the converged solution (b).

Secondly, at each point in time, the simulated force is divided by the experimental force, giving the force ratio as used in Fig. 6. For each point of strain output (time), the stress is updated by dividing the original simulation stress input by this force ratio, in order to result in updated stress–strain curves, which are used in the next set of simulations. Each set of simulations, covering five different tensile velocities, is considered an iteration.

After five iterations, the stress–strain behaviour converges to a satisfying solution, represented by the solid curves in Fig. 7 (a). The dashed lines in this figure represent the initial estimates. It shows that the converged solution does not deviate very much from the initial estimates, except for the strain rate of 5×10^{-3} s^{-1}. Fig. 7 (b) shows the comparison of the force–displacement curves for both the experimental output and the simulation output of the final solution, represented as the dashed curves. These curves of both experiment and simulation lie close enough to each other to use the stress–strain data for the design of the bulge experiment.

3.2. Free bulge pressure control

If a superplastic aluminium sheet is deformed at its optimal superplastic temperature, control over the maximum strain rate is necessary. On the other hand, the material suffers from static grain growth, because of the high temperature. Exposing the material for a long time to this temperature will result in losing superplastic properties, so the deforming time should be as small as possible. The best method to deform a sheet, keeping these points in mind, is by taking care that at each time point, this maximum strain rate will be reached. This can be achieved by prescribing the forming pressure as a function of time.

During the whole forming process, the maximum strain rate may not exceed a predefined target strain rate. In a nonlinear simulation, this can be achieved by prescribing the pressure load in the current time increment depending on the maximum strain rate in the process in the previous time increment. A user subroutine which was provided with the simulation reads the equivalent plastic strain rate at each increment at each element. This strain rate in the model is then compared with the target strain rate. The pressure on the sheet in the next increment is then a function of the ratio between the maximum equivalent plastic strain rate and the target strain rate. If the maximum equivalent plastic strain rate is higher, respectively lower than the target strain rate, then the pressure will be multiplied by a value less, respectively more than 1. This multiplication factor equals 1 in a small zone between 0.9 and 1.1 times the ratio between maximum and target strain rate.

Typical pressure–time curves, as a result from these simulations, are shown in Fig. 8, in case of sheets with an initial thickness of 1.0 mm and 0.8 mm, a bulge diameter of 70 mm and a clamping diameter of 89 mm. The target strain rate is 6×10^{-4} s^{-1}.

It must be noted here that side effects due to the different initial sheet thicknesses (0.3, 0.5, 0.8 and 1.0 mm) have been neglected. The reason for this is that the manufacturer of the material reports similar values for bulge heights reached in their experimental setup with each of these four sheet thicknesses.

4. Bulge experiments

Biaxial experiments were done by carrying out free bulge tests, where circular sheets of ALNOVI-1 were pressed with gas pressure into a cylindrical, endless die, with a diameter of 70 mm. The blanks had a diameter of 95.5 mm. The pressure–time curves are dependent on two variables: the target strain rate (6, 12 and 18 $\times 10^{-4}$ s^{-1} and the initial sheet thickness (0.3, 0.5, 0.8 and 1.0 mm). With each of these combinations, two other variables must be controlled: the maximum duration of each test and the applied backpressure during the test. Dedicated software (LabVIEW) was used to control the pressures on both sides of the sheet in order to follow the pressure–time curves as closely as possible. The setup of the bulge test will be described in more detail in the remainder of this section. Subsequently, the results of these experiments are described, in terms of reached dome heights and apex wall thickness.

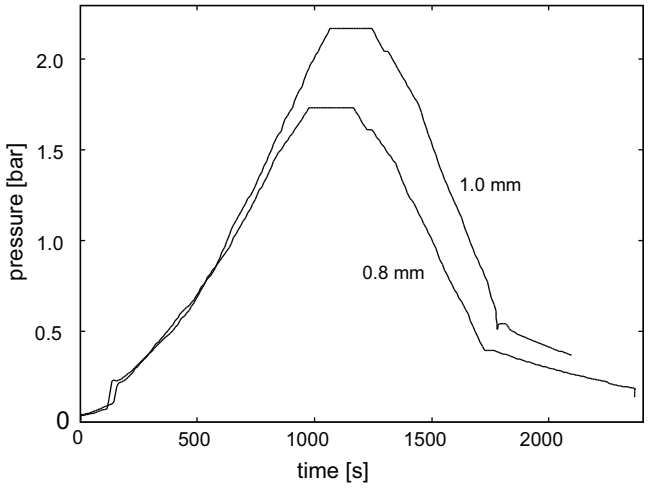

Fig. 8. Calculated pressure–time curves to be used in the free bulge experiments, target strain rate is 6×10^{-4} s^{-1}.

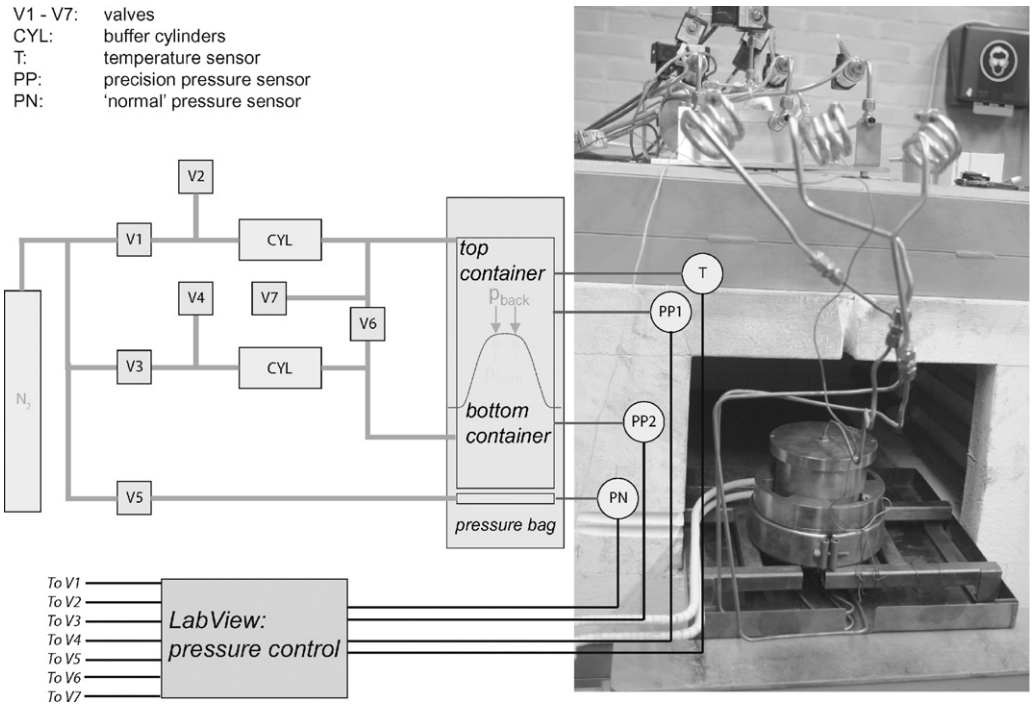

Fig. 9. Schematic and photographic view of the bulge test setup.

4.1. Bulge test setup

The setup of the test consists of two pieces. First a stainless steel container was made that was heated to the desired temperature of 520 ° C together with the blank. Secondly, a set of pressure sensors and digital valves was present, together with a LabVIEW pressure controlling program. An overview of these components is shown in Fig. 9, where it can be seen that the part which is heated inside the oven contains three pressure vessels. A cross-section of this part is shown in Fig. 10. One is the Pressure Bag, which clamps the blank (with the same time delay of 10 min as in the tensile experiments) if pressurised after reaching the desired temperature. The forming pressure is applied from within the Bottom Container. The sheet is then formed inside the Top Container. This Top Container must have the ability to be pressurised in order to apply a backpressure in the tests.

The whole sequence of steps to be taken during one experiment was programmed in the software and the program stopped if the

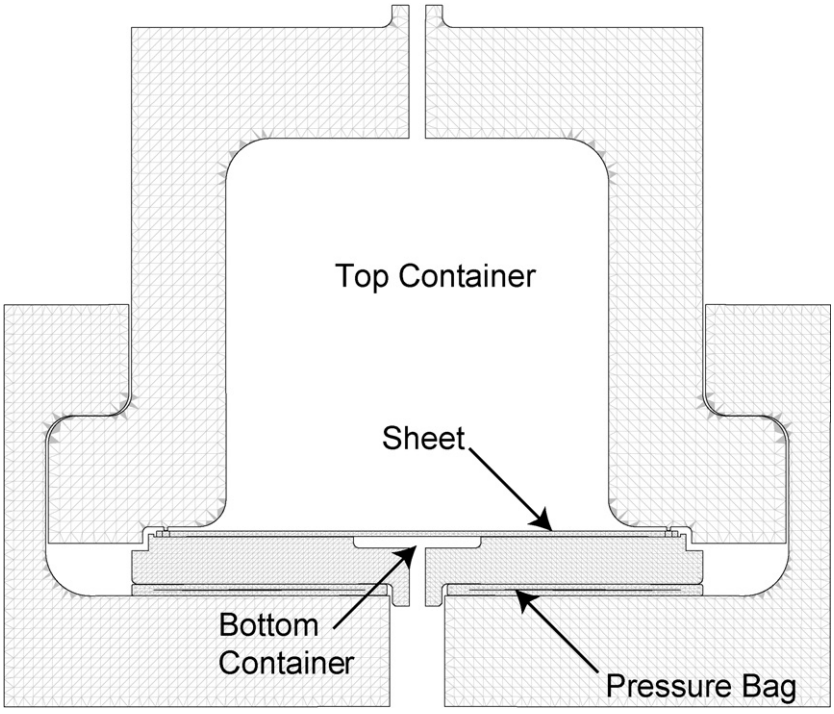

Fig. 10. Cross-section view of the three pressure vessels.

Please cite this article in press as: Q.H.C. Snippe, T. Meinders, Mater. Sci. Eng. A (2010), doi:10.1016/j.msea.2010.09.075

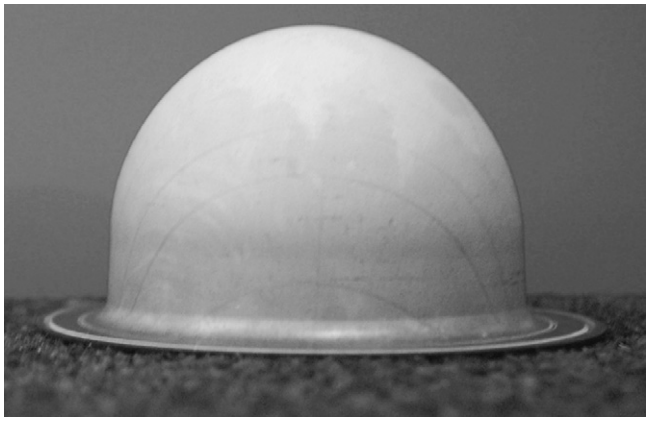

Fig. 11. Highest bulge reached in the free bulge experiments.

maximum time has been reached or if a leak has been detected, caused by failure of the material.

Three pressure sensors monitored the pressure in each of the vessels and serve as an input for the opening and closing of the digital valves. The forming pressure in time is a result of simulated curves. To be used in LabVIEW, it is most convenient to fit the curves with an expression, which uses a set of parameters to control the pressure in time. A temperature sensor monitored the temperature of the containers together with the sheet and this temperature was controlled with an extra band heater surrounding the containers. Without his band heater, the fluctuations in temperature caused by the thermostat of the furnace would be too high.

4.2. Bulge test results

The free bulging tests were mainly carried out on the sheets with an initial thickness of 1.0 and 0.8 mm. All the sheets were covered with a pencil-drawn grid (graphite), which makes it possible to measure the stretch at the top and the side of a formed bulge.

The results of the free bulging experiments are presented in terms of the obtained bulge height and resulting thickness values. A picture of the record holder in terms of reached bulge height is shown in Fig. 11.

A theoretical basis for the bulge tests can be developed, as was done by Syn et al. [26]. This theory makes use of the assumption that the thickness is the same everywhere in the model, which is clearly not the case. This was demonstrated in the work of Cornfield and Johnson [27], where the thickness distribution was made dependent on the strain rate sensitivity parameter. However, the strain rate sensitivity in this paper is independent on the strain rate, where it is known that in reality the strain rate sensitivity is highly dependent on the strain rate. The manufacturer of ALNOVI-1 reports an average value of the strain rate sensitivity of 0.5 and this value was used to predict the bulge height as function of the bulge apex thickness. Figure 5 of the paper of Cornfield shows a graph depicting the thinning factor (i.e. the pole thickness divided by the edge thickness) as function of the height-to-base-ratio (i.e. the bulge height divided by the sheet diameter). Table 4 shows the results from this analysis in terms of bulge height versus bulge apex thickness. It is assumed that the edge thickness is an average between the apex thickness and the initial thickness, since the clamping zone is situated outside the 70-mm diameter. This table shows the results in case of an initial sheet thickness of 1.0 mm. The resulting apex thickness can be linearly scaled to find the thickness at other initial sheet thicknesses. In the same table, experimental results are shown at the three different target strain rates mentioned before.

Table 4
Theoretical and measured bulge apex thickness versus bulge height, at an initial sheet thickness of 1.0 mm.

Height	10	20	30	35	40	45	49
Analytical t	0.95	0.78	0.64	0.54	0.44	0.34	0.27
Experimental t	0.97	0.73	0.54	0.42	0.34	0.24	0.18

It can be seen from the table that the theoretical values for the apex thickness are somewhat overestimated, indicating that the edge thickness assumption is not accurate enough, and/or the assumption of a strain rate independent m is insufficient. This shows that it is a complex task to predict bulge apex thicknesses as function of the bulge height.

To recall, the diameter of the bulge is 70 mm. The figure shows a bulge with a height of 53.17 mm and has been pressurised with a target strain rate of $6 \times 10^{-4}\,s^{-1}$, a backpressure of 30 bar and an initial sheet thickness of 0.8 mm.

Fig. 12(a) and (b) show plots of the bulge height versus the apex wall thickness. In Fig. 12(a) the points are categorised into different target strain rates. In Fig. 12(b), the measured points are categorised in different values for the backpressure (0, 14, 22, and 30 bar), all for sheets with an initial thickness of 1.0 mm.

From Fig. 12(a), it can be concluded that the apex wall thickness is somewhat higher for lower target strain rates at the same bulge height. This shows the high strain rate sensitivity (viscosity) of the material, where the material has more time to obtain material from

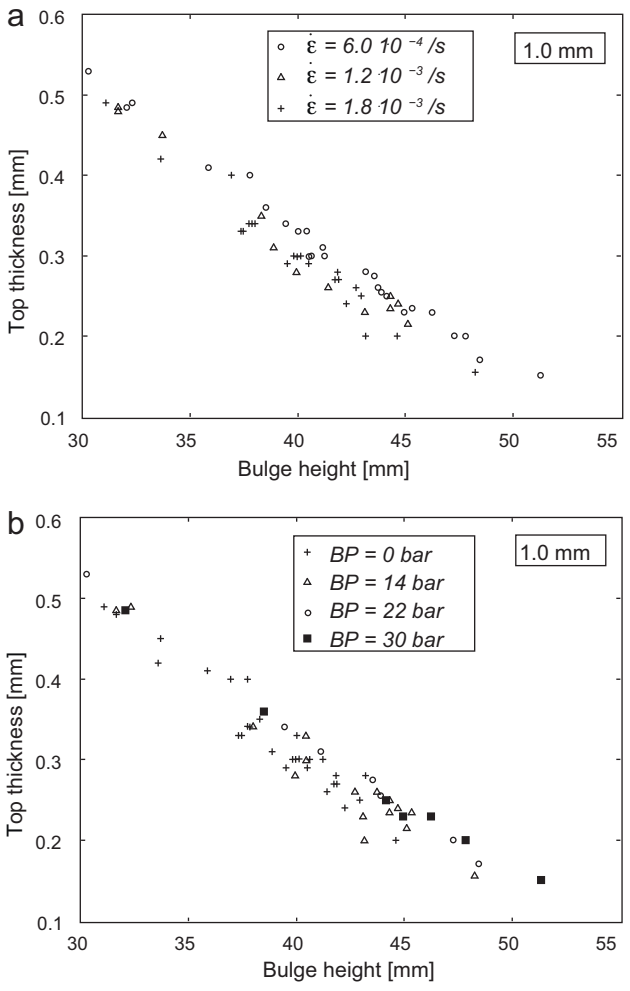

Fig. 12. Results of the free bulging experiments, top thickness vs. height (1.0 mm), per strain rate value (a), and per backpressure value (b).

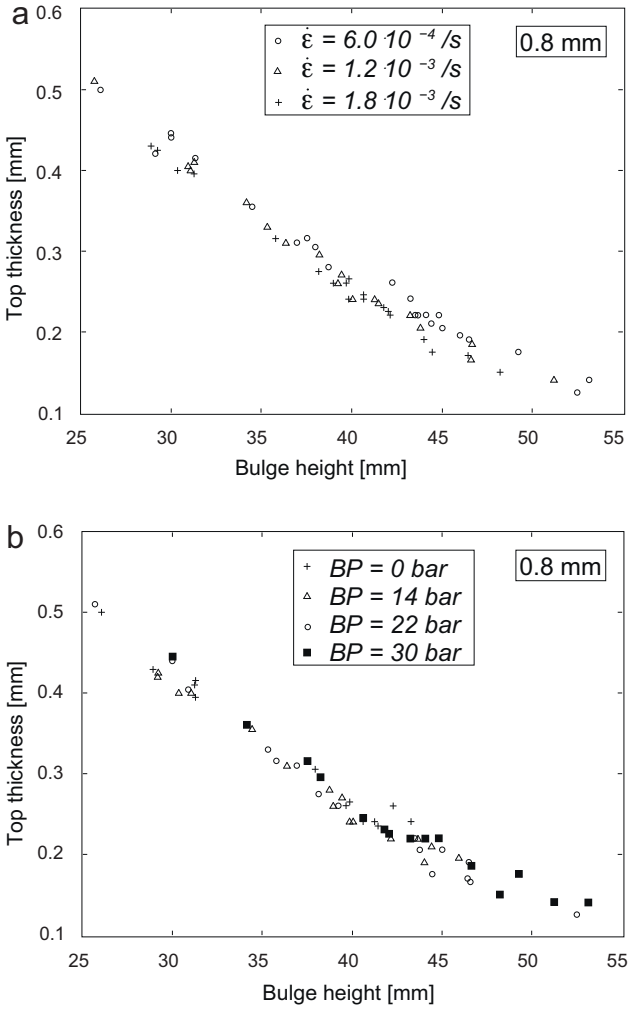

Fig. 13. Results of the free bulging experiments, top thickness vs. height (0.8 mm), per strain rate value (a), and per backpressure value (b).

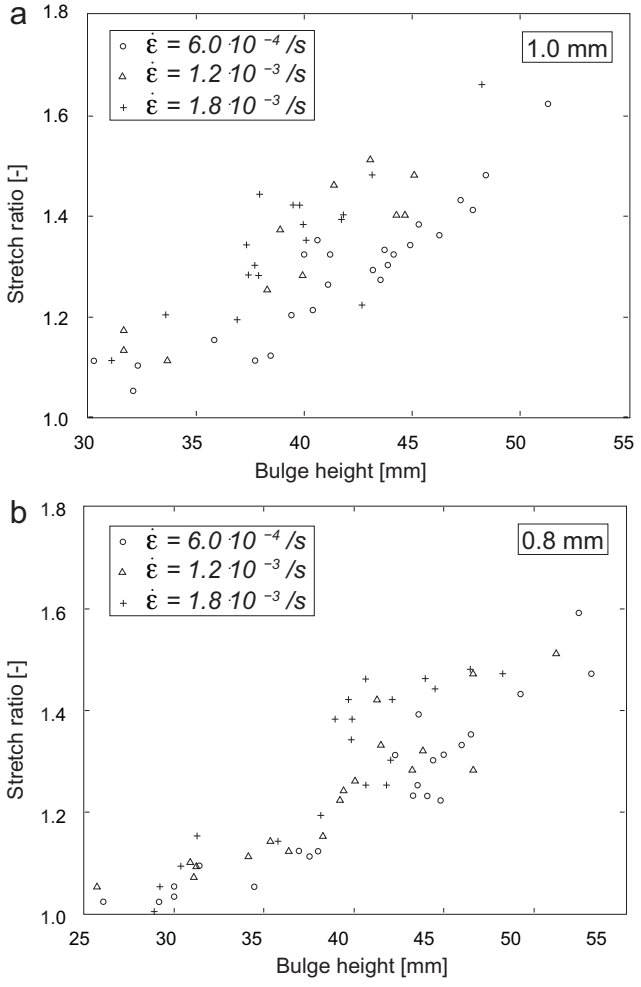

Fig. 14. Results of the free bulging experiments, stretch ratio between top and side: 1.0 mm (a) and 0.8 mm (b).

the sides to flow into the cylindrical die. From Fig. 12(b), it is clear that at higher backpressure values, higher bulges were reached. This confirms the idea that a hydrostatic pressure applied on the material inhibits the void nucleation and growth with respect to plastic strain. Fig. 13(a) and (b) show the corresponding results for the sheets with an initial thickness of 0.8 mm.

The same conclusions can be drawn for this thickness as for an initial thickness of 1.0 mm. Besides, it is observed that the maximum bulge height is the same for both thicknesses. This means that at this level of resulting apex wall thicknesses (0.15 mm), there is no influence of side effects. Also some tests were carried out on sheets with an initial thickness of 0.3 mm, with a 30 bar backpressure. These bulges also showed a bulge height exceeding 50 mm, indicating the fact that still no side effects (grain size or void size with respect to apex wall thickness) show up here.

From Fig. 12, it was concluded that at lower target strain rates, the top thickness is higher at the same bulge height. This effect is even more visible if a so-called stretch ratio r_λ is defined. This is the ratio between the measured stretch on the top of the bulge and the stretch on the side of the bulge. The stretch ratio is plotted in Fig. 14(a) and (b), in case of 1.0 and 0.8 mm initial thickness, respectively.

The most important observation in these experiments is that a high backpressure influences the maximum reachable bulge height. This is an indication that the maximum plastic strain in ALNOVI-1 before fracture is dependent on this backpressure. The stress–strain behaviour is thus dependent on the backpressure; it seems that the stress–strain curves can be thought stretched in the direction of the positive strain axis, as is schematically shown in Fig. 15.

From the grid which was drawn on the sheets, a stretch can be calculated, and thereby a value for the equivalent plastic strain. For each of the target strain rate values and each of the backpressure values, the bulge with the maximum height was used to determine the equivalent plastic strain, the results are shown in Table 5.

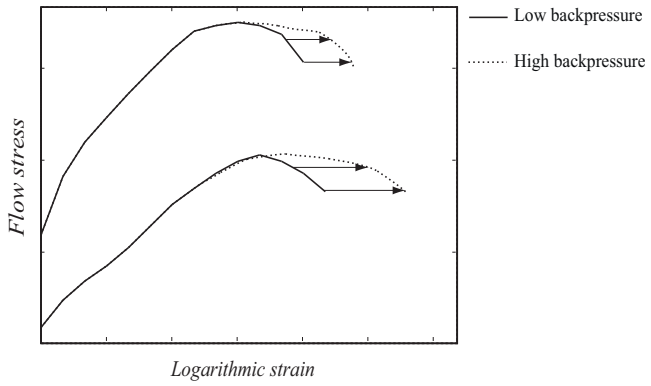

Fig. 15. Schematic view of stretched stress–strain curves depending on hydrostatic pressure.

Please cite this article in press as: Q.H.C. Snippe, T. Meinders, Mater. Sci. Eng. A (2010), doi:10.1016/j.msea.2010.09.075

Table 5
Maximum values for the equivalent plastic strain, as calculated from the grid lines drawn on the specimens. The maximum values are presented as function of the target strain rate and the applied backpressure during forming.

Target strain rate	0	14	22	30
6×10^{-4}	1.25	1.42	1.66	1.81
12×10^{-4}	1.23	1.47	1.57	1.77
18×10^{-4}	1.30	1.39	1.56	1.61

5. Leak testing

All formed cups from the free bulging experiments have been leak tested in an experimental setup. Within this setup, the outer side of the cup was drawn vacuum, while the inner side was filled with helium at atmospheric pressure. The leak through the formed sheet was then measured with an Alcatel ASM 181 td Leak Detector.

The experimental setup must be designed such that it can be attached to the leak detector by means of a standardised vacuum flange. This should be at the side of the formed cup which should be made vacuum. The other side of the formed cup must be flushed with helium. It must be ensured that because of the overpressure of 1 bar at the inside, the material does not undergo plastic deformation. This was done by measuring the bulge height before and after the leak test, and this did not result in any height differences. Leak rate is expressed in the unit mbar l s^{-1} He. This unit represents the amount of helium (mbar l) traversing the formed sheet per time unit. The leak tester does neither 'know' about the geometry to be tested, nor the pressure difference between the two sides of this geometry (Fig. 16).

The results of the leak experiments can, just as with Fig. 12, be categorised in target strain rate or in backpressure. Since a high backpressure is thought to postpone void nucleation and growth behaviour, the latter categorisation is the most interesting. Table 6 shows the highest bulges at each backpressure value for two different leak rates: first, a leak rate just above the minimum rate which could be measured (10^{-8} mbar l/s); secondly, the highest value of the leak rate below 10^{0} mbar l/s, since this is a value at which no holes are visible in the bulge. If holes were already visible with the bare eye, these bulges were not leak-tested, since this would result in an absurdly high leak value. Bulges with visible holes were all categorised under a leak value of 10^{0} mbar l/s. From this table it can be concluded that a higher backpressure has a beneficial effect on the leak rate. Secondly, it seems that a low leak value is less dependent on the initial sheet thickness than a high leak value.

As was mentioned in the abstract, leak tightness is, in this case, a very important parameter. The application of a backpressure in the forming stage, which has a value in the order of the flow stress of the material, can therefore be crucial when manufacturing complex 3D-shaped thin-walled detector parts.

6. Conclusion/future work

Mechanical experiments on the superplastic aluminium alloy ALNOVI-1 show that the conditions for optimal superplasticity occur at a temperature of 520° C and a low strain rate, which is about 1.2×10^{-3} s^{-1}. From the tensile experiments it is clear that the response in terms of stress versus strain is very sensitive to the strain rate, i.e. the material shows a high strain rate sensitivity.

The force–displacement results from the tensile experiments are used to construct stress–strain curves, by means of an inverse modelling procedure. Also, the void volume fractions were investigated, which shows a strong dependence on the plastic strain but not on the plastic strain rate.

Using the stress–strain curves at different strain rates, a routine was written to analyse the pressure which was needed in order to maintain a maximum strain rate in the bulge experiments. The maximum height which was reached in the bulge experiment, without applying a backpressure, was about 40 mm, independent of the target strain rate. But with a backpressure of 30 bar applied, bulges higher than 50 mm were possible. Also, application of a backpressure resulted in bulges which show a better leak tightness at the same bulge height. So, a backpressure influences the results in a positive way.

Future work

The results of both experiments are used to construct a user-defined material model to be used in ABAQUS/Standard. The purpose of this model is to simulate the superplastic manufacturing process of these complex 3D products. From this material model, it should be possible to predict the amount of leak of a formed sheet. Also, a more general form of the von Mises yield criterion can be

Table 6
Overview of the highest bulges with a leak rate as defined in the table, expressed in mm and mbar l/s, respectively. The bulge heights are presented as dependent on the applied backpressure (BP; in bar) and the initial sheet thickness, 0.8 and 1.0 mm.

BP		0	14	22	30
Leak 10^{-8}	0.8 mm	31.31	34.47	39.23	44.82
	1.0 mm	31.67	37.97	39.43	46.26
Leak 10^{-1}	0.8 mm	37.97	40.04	46.50	49.24
	1.0 mm	41.85	42.69	47.27	51.32

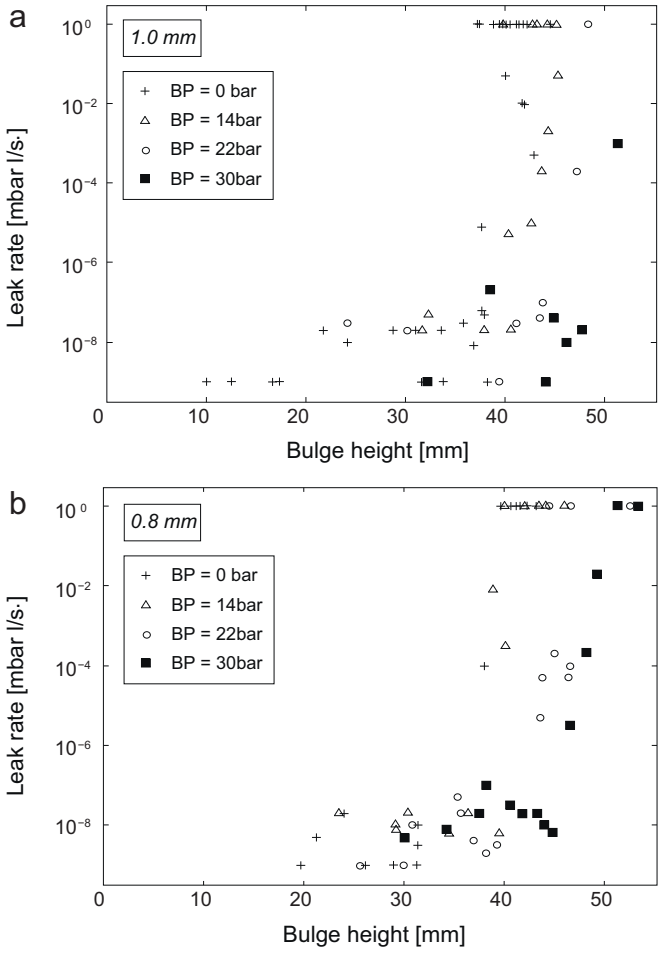

Fig. 16. Leak test results of the formed cups, leak rate vs. bulge height, by backpressure value, at an initial thickness of (a) 1.0 mm and (b) 0.8 mm.

implemented, which is common for aluminium alloys at elevated temperatures (e.g. the Hosford yield criterion).

References

[1] K. Padmanabhar, R. Vasin, F. Enikeev, Superplastic Flow: Phenomenology and Mechanics, Springer, 2001.
[2] N. Ridley, P.S. Bate, B. Zhang, Mater. Sci. Eng. A 410–411 (2005) 100–104.
[3] D.H. Bae, A.K. Ghosh, Acta Mater. 50 (2002) 993–1009.
[4] P.K.D.V. Yarlagadda, P. Gudimetla, C. Adam, J. Mater. Process. Technol. 130–131 (2002) 469–476.
[5] N. Chandra, Int. J. Non-Linear Mech. 37 (2002) 461–484.
[6] D.H. Bae, A.K. Ghosh, Acta Mater. 50 (2002) 1011–1029.
[7] M.A. Khaleel, H.M. Zbib, E.A. Nyberg, Int. J. Plasticity 17 (2001) 277–296.
[8] R.A. Vasin, F.U. Enikeev, M. Tokuda, R.V. Saffiulin, Int. J. Non-Linear Mech. 38 (2003) 799–807.
[9] Y. Chen, K. Kibble, R. Hall, X. Huang, Mater. Des. 22 (2001) 679–685.
[10] A.H. Chokski, Mater. Sci. Eng. A 410–411 (2005) 95–99.
[11] F.A. Mohamed, Surf. Interface Anal. 31 (2001) 532–546.
[12] R.A. Vasin, F.U. Enikeev, M.I. Mazurski, O.S. Munirova, J. Mater. Sci. 35 (2000) 2455–2466.
[13] Furukawa Sky Aluminium Corp., Furukawa Review 26: Superplastic Aluminium Alloy Sheet "ALNOVI-1" was Approved by Airbus (2004).
[14] General Motors, Bulge Test for Quick Plastic Forming, GM Standard GMN11198 (2005).
[15] Y. Luo, C. Miller, G. Luckey, P. Friedman, Y. Peng, J. Mater. Eng. Perform. 16 (2008) 274–283.
[16] S. Mahabunphachai, M. Koç, Int. J. Mach. Tools Manuf. 48 (2008) 1014–1029.
[17] Z.P. Chen, P.F. Thompson, J. Mater. Process. Technol. 148 (2004) 204–219.
[18] F. Jovane, Int. J. Mech. Sci. 10 (1968) 403–427.
[19] F.U. Enikeev, A.A. Kruglov, Int. J. Mech. Sci. 37 (5) (1995) 473–483.
[20] S.G. Luckey, P.A. Friedman, K.J. Weinmann Jr., J. Mater. Process. Technol. 194 (2007) 30–37.
[21] M.H. Hojjati, M. Zoorabadi, S.J. Hosseinipour, J. Mater. Process. Technol. 205 (2008) 482–488.
[22] D.H. Bae, A.K. Ghosh, Acta Mater. 50 (2002) 993–1009.
[23] R.M. Cleveland, A.K. Ghosh, J.R. Bradley, Mater. Sci. Eng. A A351 (2003) 228–236.
[24] A.H. Chokshi, A.K. Mukherjee, Mater. Sci. Eng. A A171 (1993) 47–54.
[25] J. Hedworth, M.J. Stowell, J. Mater. Sci. 6 (1971) 1061–1069.
[26] C.K. Syn, M.J. O'Brien, D.R. Lesuer, O.D. Sherby, An Analysis of Gas Pressure Forming of Superplastic AL5083 Alloy, Lawrence Livermore National Laboratory, 2001, ref. UCRL-JC-135190.
[27] G.C. Cornfield, R.H. Johnson, Int. J. Mech. Sci. 12 (1970) 479–490.

Please cite this article in press as: Q.H.C. Snippe, T. Meinders, Mater. Sci. Eng. A (2010), doi:10.1016/j.msea.2010.09.075